22nd International Conference on Renewable Energies and Power Quality (ICREPQ'24)
Bilbao (Spain), 26th to 28th June 2024

ISBN: 978-84-09-60656-6

Optimizing Wireless Power Systems: Comparative Analysis of Electronic Converters and Techniques

Hassan Ali Hussein [1], Ali Jafer Mahdi [1, 2] and Manal Hussein Nawir [1]

[1] *Department of Electrical and Electronics Engineering, University of Kerbala, Karbala 56001, Iraq*

[2] *College of Information Technology Engineering, Al-Zahraa University for Women, 56001 Karbala, Iraq.*

Abstract. This research aims to advance wireless power transfer (WPT) technology, focusing on increasing efficiency and transmission distance between the sending and receiving coils. The paper will explore the utilize of advanced power-electronic converters for converting direct current to alternating current with maximum power transfer, this assessment was conducted on three distinct categories of inverters, namely class-E, class-D, and H-bridge, in order to establish a comparison among them based on the identical parameters of the system. After formulating the proposed system, a simulation using matlab has been conducted for distances that vary across three variables. From the outcomes of this simulation, it has been determined that the class-E inverter exhibits the highest level of efficiency and power transfer in relation to the suggested battery charging system.

Key words. Wireless power transfer (WPT), Inductive coupling wireless power transfer (ICWPT), electric vehicle (EV).

1. Introduction

Wireless power transfer (WPT) facilitates a convenient and more secure method of providing power, which offers commendable efficiency and reliability. The emergence of various significant obstacles has been observed as a result of the implementation of cable charging mechanisms in electric automobiles, including the potential hazards associated with worn cables that may pose a risk of electric shock, as well as the possibility of forgetting to establish a proper connection with the charging plug. Despite the undeniable advantages that wireless power transfer brings to the table in terms of simplicity and flexibility for charging electric vehicles, it is crucial to recognize the substantial reduction in power and efficacy that could arise due to diverse factors including the notable separation between the sender and receiver, alignment concerns, and potential alterations in the transmission distance based on the specific circumstances of the original system design[1],[2], the utilization of wireless power presents the opportunity for connector-free devices, thereby enhancing both the size and reliability[3]. With respect to the distance over which power is transmitted, wireless power transfer (WPT) can be classified into two primary categories: far-field transmission and near-field transmission. The inductive power transfer (IPT), capacitive power transfer (CPT), and permanent magnet coupling (PMC) represent the most widely utilized near-field wireless power transfer (WPT) technologies[4],[5]. In the realm of interconnected resonances (for instance, acoustic, electromagnetic, magnetic, nuclear), a state of operation known as "strong coupling" is established, resulting in the ability to efficiently transfer energy. The implementation of mid-range wireless power transfer, guided by the principles of this robust coupling theory, yields a nearly unidirectional and highly efficient transmission with minimal disruptions and energy losses[6], Electric power is transferred via electromagnetic induction between the transmitter and receiver coils. The effectiveness of this transfer is defined by the coupling factor, which is closely associated with the gap distance between the transmitting and receiving coils, and is also influenced by any misalignment between them[7]. A two-coil system is the term used to describe a transformer with leakage inductances that are loosely coupled and requires the use of compensation topologies. Some of the primary compensation topologies include SS, SP, PP, and PS[8]. The design of wireless pads, compensation topologies, and several power electronics converters are all covered in a large number of literary works. power-transfer efficiency of 84.4% was attained with a total output power of 5.7 W, the class-E ZVS/ZDS allowed the suggested system to maintain excellent power conversion efficiency[9]. An efficient design factor for high power WPT applications, such EV charging, with HF voltage source H-bridge inverters[10], A RIC-WPT system operating at a frequency of 1 MHz, with a class-E inverter and class-DE rectifier was able to attain a total efficiency of 73.0%. The system delivered an output power of 9.87 W (50 Ω) and the coil distance was set at 10 cm[11]. These works have put considerations for the proposed system. In contrast to what has been presented in the existing literature, this paper aims to design and conduct a comparative analysis among three types of inverters. The objective is to select the most efficient invertir for proposed WPT system, while simultaneously increasing the efficiency and distance between the coils.

2. System Description of ICWPT

The proposed system as shown in (Figure 1) is comprised of an AC voltage source with a magnitude of 220V and a frequency of 50Hz. Additionally, a power transformer is employed for the purpose of reducing the voltage level from 220V to 110V in order to supply the (AC-DC) bridge rectifier, which is equipped with a capacitor filter. This allows for the control of the system through the use of a (DC-DC) step down buck converter.

By manipulating the duty cycle of the MOSFET, the amplitude of the voltage can be regulated. Consequently, power can be transferred through inductive coupling, requiring the use of AC power. To achieve this, a power electronic (DC-AC) inverter is employed. Within this research, three types of inverters are implemented in the system, namely class E, class D, and H-bridge inverters. The coupling coils in the system serve as the transmitter and receiver, and they are accompanied by the S-S compensation network. Additionally, a bridge rectifier (AC-DC) converter, equipped with a capacitor filter, is responsible for supplying the load with DC voltage.

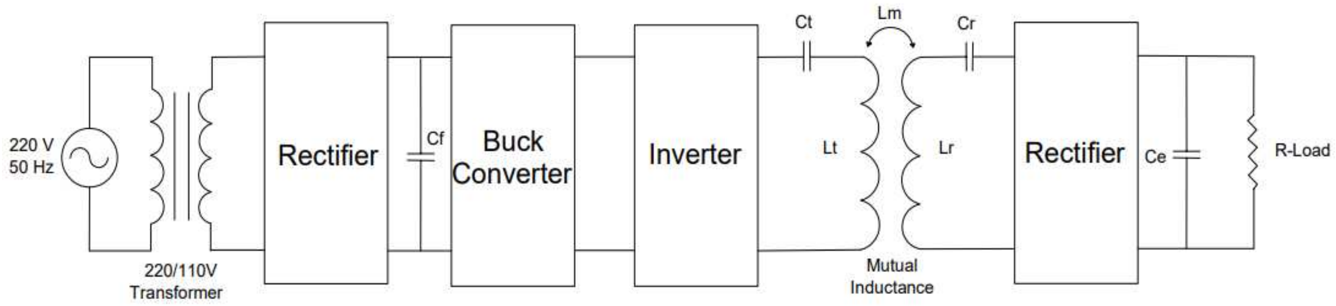

Figure 1. Typical block diagram of proposed ICWPT system.

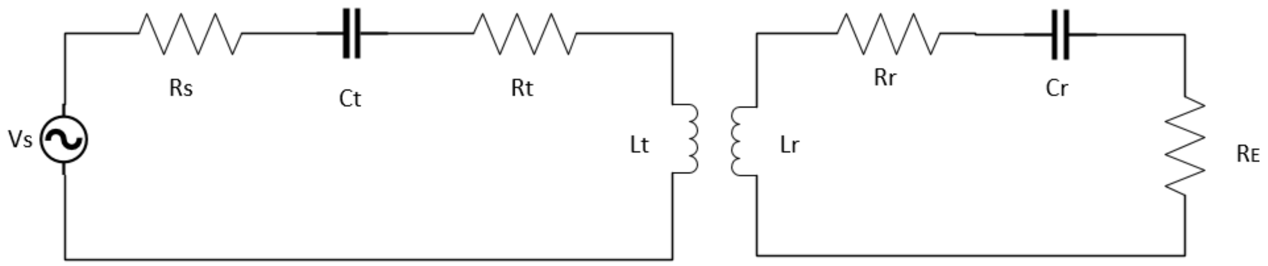

Figure 2. Equivalent ideal circuit of ICWPT system.

3. Design of Proposed ICWPT System

Designing the parameters of the main parts of ICWPT system (coils and compensation network, buck converter, DC-AC inverters).

A. Coil Design

There exist diverse coil structures that have been devised with the sole objective of enhancing the mutual coupling and efficiency of the inductive link. The physical structure, geometry, and placement of the coils play crucial roles in determining the self-inductance, mutual inductance, parasitic equivalent resistance, and transmission efficiency of each individual coil. Among the coil structures widely employed in electric vehicle (EV) applications, the circular spiral configuration is particularly favored due to its favorable power transmission performance and ability to tolerate misalignment[12].

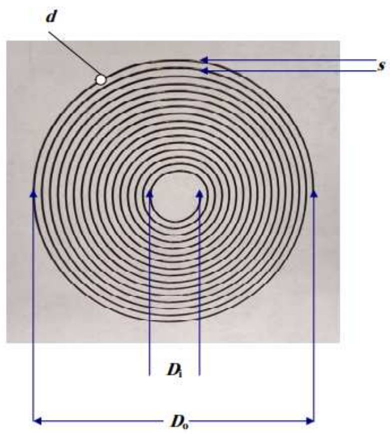

Figure 3. Real printed wireless coil by CNC machine.

In the context of a circular spiral coil, the parameter R represents the outer radius, N1 denotes the number of turns in the Transmitter coil, N2 signifies the number of turns in the Receiver coil, D_O stands for the outer diameter of the coil in millimeters, S refers to the spacing between two turns in millimeters, Di indicates the inner diameter of the coil in millimeters, and d represents the diameter of the wire coil in millimeters.

$$M = K\sqrt{L1 * L2} \tag{1}$$

$$W1 = \frac{1}{\sqrt{L1 * C1}} \tag{2}$$

$$W2 = \frac{1}{\sqrt{L2 * C2}} \tag{3}$$

The mutual inductance denoted by M represents the interaction between the primary and secondary coils, while the coupling coefficient is denoted by K. Resonance frequencies of the primary and secondary are represented by W1 and W2, respectively. Additionally, the primary and secondary inductances are denoted by L1 and L2, and the primary and secondary capacitances are denoted by C1 and C2. The flat spiral coils were constructed with an outer diameter measuring 260 mm and an inner diameter of 50 mm. These coils were wound with 16 turns, each spaced by 5 mm gaps. In order to achieve these specific diameters, a 9-meter length of copper wire, possessing a circular cross section with a diameter of 2 mm, was utilized to form the coils.

B. Buck Converter Design

Buck converters, which are commonly employed in power electronics applications for direct current voltage conversion, decrease the input direct current voltage based on the duty cycle. These converters are extensively utilized. Their significant benefits encompass the ability to be designed for high power applications, exhibit high efficiency, and possess a favorable price-performance ratio. The generation of output voltage by buck converters is facilitated through the implementation of pulse width modulation techniques (PWM)[13]. (Figure 4) shows the basic structure of buck converter.

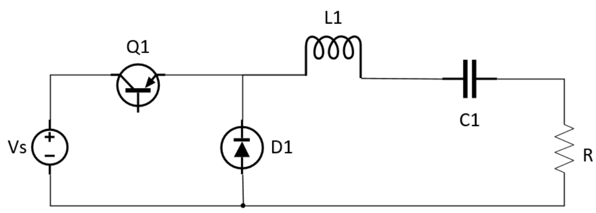

Figure 4. Buck converter basic circuit diagram.

The conversion ratio can be calculated by (4):

$$V_O = D * V_S \tag{4}$$

Where D is the duty cycle of buck converter.
The following formula(5) can be used to determine the minimum inductance (L_{min}) value needed for the converter to function in continuous current mode:

$$L_{\min} = \frac{(1 - D) * R}{2 * F} \tag{5}$$

Switching frequency of the circuit is denoted by F

The voltage ripple of the output in a buck converter should typically be below 1%. As the ripples in the current of the inductance are also observed in the current of the capacitor, the value of the capacitor can be determined in order to achieve the desired output voltage ripple (ΔV0 / V0). This calculation can be made by(6) to ensure that the ripple is at the desired level:

$$C_O = \frac{(1 - D)}{8L(\Delta V_O / V_O)F^2} \tag{6}$$

The circuit design criteria and parameters were utilized to establish the values of circuit elements in a simple buck converter running in continuous current mode.

C. Class-E Inverter Design

Designing the inverter parameters shown in(Figure 5) for 25Ω resistive load, that represent (Electric Bicycle Battery, 48V, 20AH Lithium Li-ion Battery accompanied by a 4A Charger, suitable for E-Bike Kits with power ratings of 1000W/1500W) with a fixed charging current 2A.The examination of the circuit required for enabling wireless charging of the electric vehicle that was designed has been carried out in the present section. The determination of the most favorable operating conditions has been achieved through the calculation of the components of the Class-E inverter utilized as a power supply with high frequency. The analysis of the fluctuation in mutual inductance among the coils within the Wireless Power Transfer (WPT) arrangement has been investigated. The analysis of impedance, encompassing the entirety of the system[1].

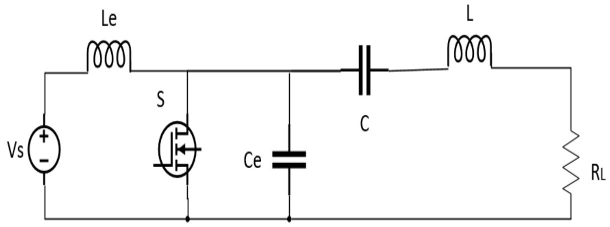

Figure 5. Circuit topology of class-E inverter.

To compute the inverter parameters, various crucial variables must first be obtained, such as the impedance reflected from the receiver side to the transmitter side, indicating an influence on the transmitter impedance.
By Finding the equivalent resistance R_L as[14]:

$$R_L = R_O \frac{8}{\Pi^2} \tag{7}$$

The currents passing through the receiver and transmitter coils are denoted as I_R and I_T, respectively:

$$I_T = \frac{I_R(R + R_L)}{-j2\Pi FM} \tag{8}$$

To calculate the loading impact (reflected impedance) of the receiver on the transmitter side, as follows:

$$Z_{ref} = \frac{W^2 M^2}{(R + R_L)} \tag{9}$$

The total resistance of the transmitter side (Z_T) describes the power amplifier's load resistance as follows:

$$Z_T = Z_{ref} + R_T \tag{10}$$

Finding the equivalent inductance L_{eq} as:

$$L_{eq} = \frac{1.1525 Z_T}{W} \tag{11}$$

The inductance of the transmitter coil L_T is divided into two parts are Lx and Leq:

$$L_X = L_T - L_{eq} \tag{12}$$

Finding the compensation capacitance C_T as:

$$C_T = \frac{1}{L_X * W^2} \tag{13}$$

Finding the shunt capacitor Ce as:

$$C_e = \frac{0.1836}{W * Z_T} \tag{14}$$

The choke-inductor (Le) must be large enough to pass a DC current as in (15):

$$L_e = 3.5 \frac{Z_T}{F} \tag{15}$$

Finaly the efficiency of WPT system can be reached as:

$$\eta = \frac{W^2 M^2 R_L}{(R_1 + R_L)^2 (R_T + Z_{ref})} \tag{16}$$

D. Class-D Inverter Design

The configuration of an enhanced Class D ZVS invertir demonstrated in (Figure 6), comprises of dual bidirectional switches, specifically denoted as S1 and S2, in conjunction with a series-resonant LCR circuit and a parallel-connected capacitor Cs. These aforementioned switches, S1 and S2, are constructed using power MOSFETs, paired with antiparallel diodes. The direct current (DC) voltage source behaves akin to a short circuit for the alternating current (AC). As a result, the inherent capacitances of both switches are linked in parallel to the ac signal. Through the utilization of rectangular voltages and a sufficiently prolonged dead time, the switches are cycled alternately. Additionally, the operational duty cycle of each driving voltage does not exceed 0.5[15].

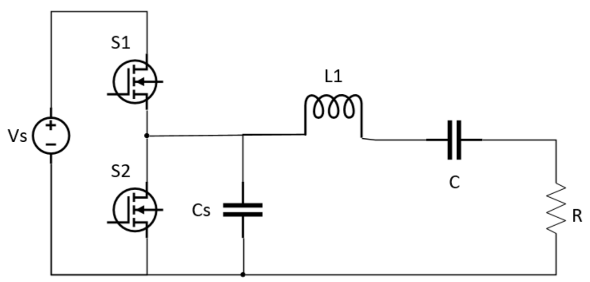

Figure 6. Circuit diagram of class-D ZVS inverter.

E. H-Bridge Inverter Design

In a full bridge inverter configuration four power switches (typically MOSFETs or IGBTs) are arranged in a bridge configuration. The switches are controlled in such a way that they generate an alternating current (AC) waveform at the desired frequency and voltage. The AC waveform is then used to induce a magnetic field in a transmitting coil, which in turn transfers power wirelessly to a receiving coil[16].

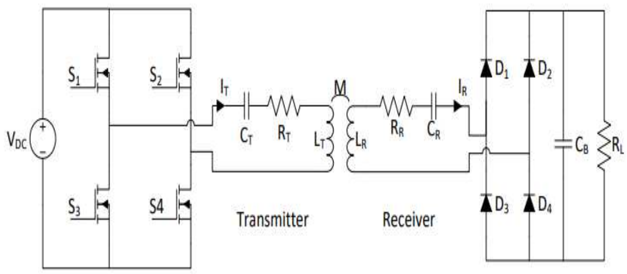

Figure 7. ICWPTS with H-bridge inverter

R_T and R_R denote the losses experienced in both the transmitter and receiver resonators, encompassing the resistance of the coil and the resistance encountered in the series of capacitors.

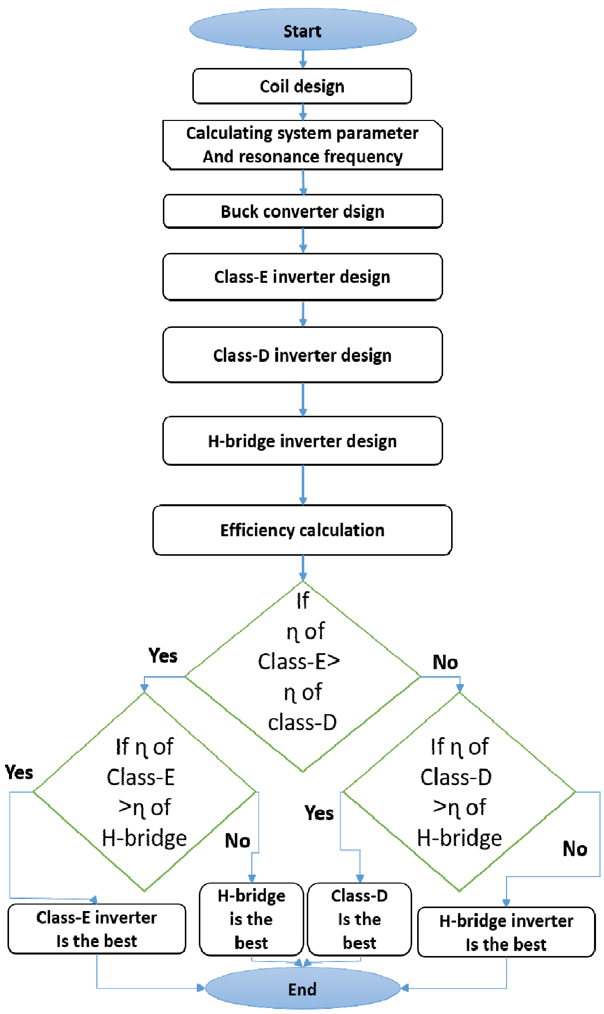

Figure 8. Flow chart depicting the process of designing WPT and a comparison of inverters.

4. Simulation results

After the meticulous design and thorough analysis of each component within the Wireless Power Transfer (WPT) system, and by calculating the transfering efficiency of the equivelant circuit of the system(Figure 2), as well as the assessment of three distinct inverters for the purpose of implementing the WPT system, a comprehensive simulation was conducted using MATLAB. The objective of this simulation was to assess the overall efficiency of the system when utilizing these three inverters, as well as to determine the coupling coefficient and power transfer efficiency for several distances between the transmitter and receiver coils (10, 13 and 16) cm. These measurements enable a comparison of the inverters' performance within the same proposed circuit across different working scenarios. All results shown in (Figure 18).

A. *WPT system with class-E invertir*

Table 1.- simulation results and calculated efficiency for WPT system with class-E inverter.

d(cm)	K	Pin (W)	Pout (W)	Simulated system ɳ (%)	Calculated equivelant circuit ɳ (%)
10	0.498	109.7	102.8	93.7	96.7
13	0.353	112.2	102.8	91.68	93.4
16	0.25	121.5	102.7	84.54	88.1

B. *WPT system with class-D invertir*

Table 2.- simulation results and calculated efficiency for WPT system with class-D inverter.

d(cm)	K	Pin (W)	Pout (W)	Simulated ɳ (%)	Calculated equivelant circuit ɳ (%)
10	0.498	110	102.8	92.63	96.7
13	0.3536	118.8	102.7	86.43	93.4
16	0.25	134.1	102.3	76.28	88.1

C. *WPT system with H-bridge invertir*

Table 3. - simulation results and calculated efficiency for WPT system with H-bridge inverter.

d(cm)	K	Pin (W)	Pout (W)	Simulated ɳ (%)	Calculated equivelant circuit ɳ (%)
10	0.498	111.1	102.6	92.37	96.7
13	0.3536	118.7	102.3	86.21	93.4
16	0.25	134.7	102.6	76.18	88.1

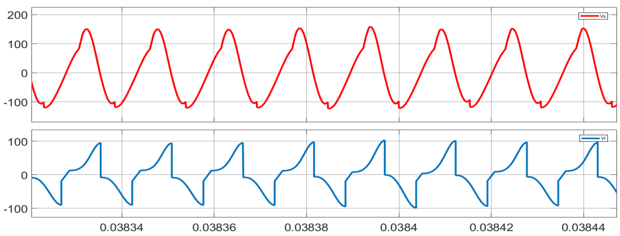

Figure 9. Vs &Vr waveforms for WPTS with Class-E inverter and d=10cm.

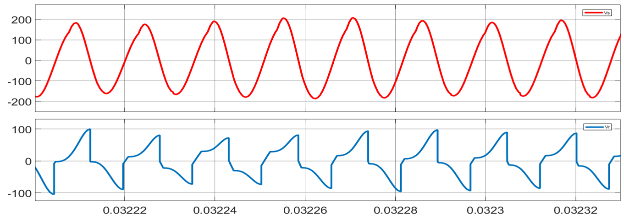

Figure 10. Vs &Vr waveforms for WPTS with Class-E inverter and d=13cm.

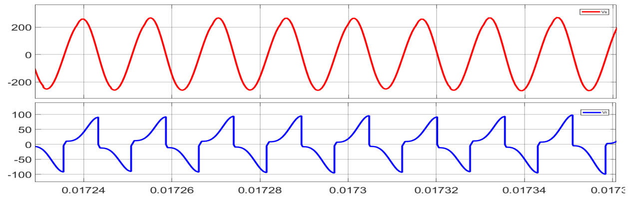

Figure 11. Vs &Vr waveforms for WPTS with Class-E inverter and d=16cm.

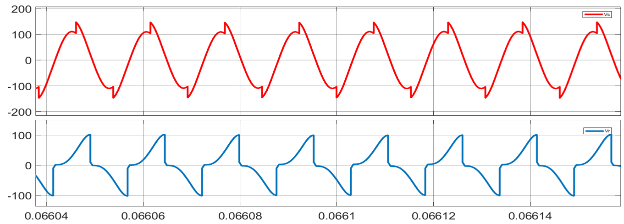

Figure 12. Vs &Vr waveforms for WPTS with Class-D inverter and d=10cm.

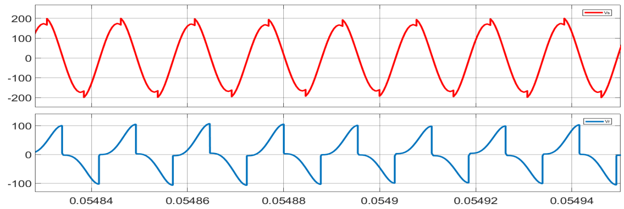

Figure 13. Vs &Vr waveforms for WPTS with Class-D inverter and d=13cm.

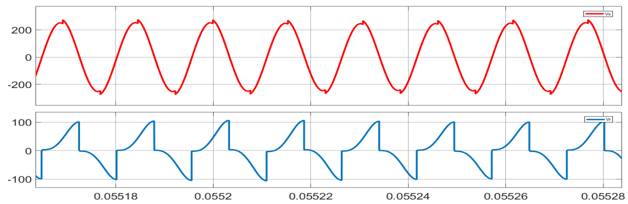

Figure 14. Vs &Vr waveforms for WPTS with Class-D inverter and d=16cm.

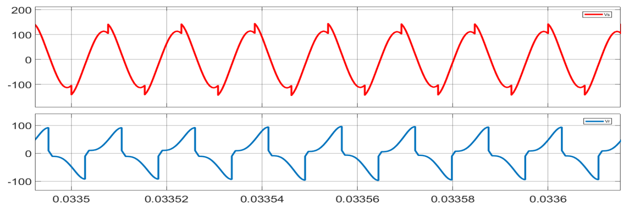

Figure 15. Vs &Vr waveforms for WPTS with H-bridge inverter and d=10cm.

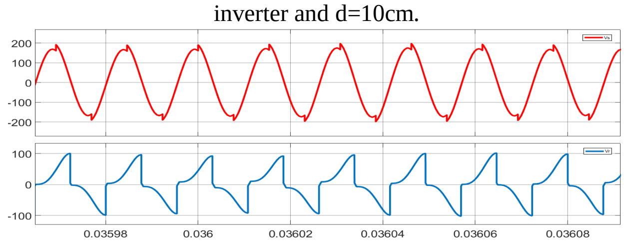

Figure 16. Vs &Vr waveforms for WPTS with H-bridge inverter and d=13cm.

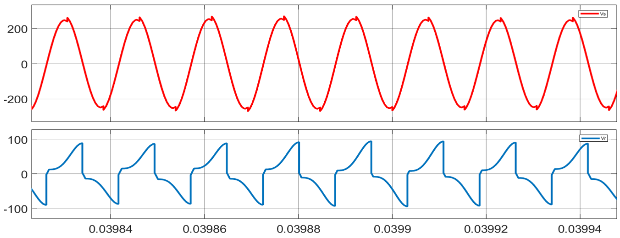

Figure 17. Vs &Vr waveforms for WPTS with H-bridge inverter and d=16cm.

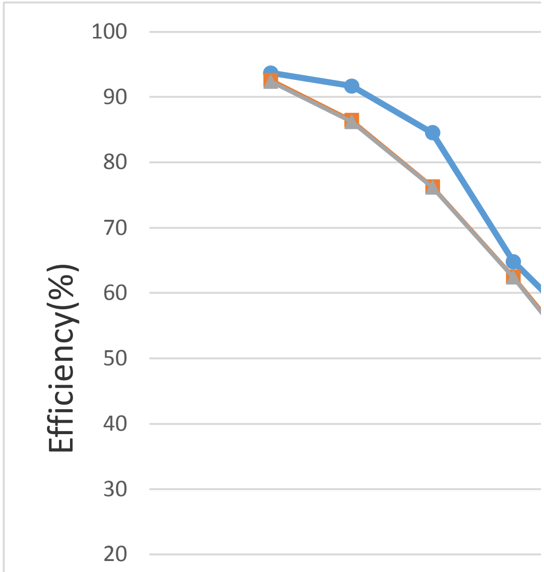

Figure 18. The correlation between efficiency and the variation in distance between the two coils in (WPT) system.

Future work

Implementing the ICWPT system which utilizes a transmitter equipped with a class-E inverter. Additionally, integrating Artificial Intelligent Algorithms (AIA) is employed to optimize the resonance circuit's frequency in order to further enhance the system's overall performance.

4. Conclusion

After the design, analysis, and simulation of the proposed Wireless Power Transfer (WPT) system for battery charging application, as well as the development of three proposed inverters for integration into the system, the overall efficiency of the system has been determined. This evaluation was carried out for each inverter type (class-E, class-D, and H-bridge) and for varying distances between the transmitter and receiver coils (10 cm, 13 cm and 16 cm). The efficiency calculations took into account the coupling coefficient and mutual inductance for each specific scenario. For a separation of 10 centimeters, the overall effectiveness of the wireless power transfer (WPT) system reached 93.7% when employing a class-E inverter. Conversely, when utilizing a class-D inverter, the efficiency dropped to 92.63%, while with an H-bridge inverter, it decreased even further to 92.37%. Based on the results it can be concluded that the system equipped with the class-E inverter exhibited the highest efficiency and the most power transferred compared to the other two inverters. This finding holds true for all three cases, where the parameters of the system were kept constant.

References

[1] F. Issi and O. Kaplan, “Design and application of wireless power transfer using Class-E inverter based on Adaptive Impedance-Matching Network,” *ISA Trans.*, vol. 126, pp. 415–427, 2022.

[2] Q. Li, S. Duan, and H. Fu, “Analysis and Design of Single-Ended Resonant Converter for Wireless Power Transfer Systems,” *Sensors*, vol. 22, no. 15, p. 5617, 2022.

[3] S. Ansari, A. Das, and A. Bhattacharya, “Resonant inductive wireless power transfer of two-coil system with class-e resonant high frequency inverter,” in *2019 6th International Conference on Signal Processing and Integrated Networks (SPIN)*, IEEE, 2019, pp. 269–273.

[4] M. Etemadrezaei, “Wireless power transfer,” in *Power Electronics Handbook*, Elsevier, 2018, pp. 711–722.

[5] F. Corti, A. Reatti, Y.-H. Wu, D. Czarkowski, and S. Musumeci, “Zero voltage switching condition in class-e inverter for capacitive wireless power transfer applications,” *Energies*, vol. 14, no. 4, p. 911, 2021.

[6] S. Das Barman, A. W. Reza, N. Kumar, M. E. Karim, and A. B. Munir, “Wireless powering by magnetic resonant coupling: Recent trends in wireless power transfer system and its applications,” *Renew. Sustain. energy Rev.*, vol. 51, pp. 1525–1552, 2015.

[7] A. J. Mahdi, S. Fahad, and W. Tang, “An adaptive current limiting controller for a wireless power transmission system energized by a PV generator,” *Electronics*, vol. 9, no. 10, p. 1648, 2020.

[8] Z. Bi, T. Kan, C. C. Mi, Y. Zhang, Z. Zhao, and G. A. Keoleian, “A review of wireless power transfer for electric vehicles: Prospects to enhance sustainable mobility,” *Appl. Energy*, vol. 179, pp. 413–425, 2016.

[9] H. Sekiya *et al.*, “Loosely coupled inductive wireless power transfer systems with class-E transmitter and multiple receivers,” in *2014 IEEE Energy Conversion Congress and Exposition (ECCE)*, IEEE, 2014, pp. 675–680.

[10] A. A. S. Mohamed, D. Allen, T. Youssef, and O. Mohammed, “Optimal design of high frequency H-bridge inverter for wireless power transfer systems in EV applications,” in *2016 IEEE 16th International Conference on Environment and Electrical Engineering (EEEIC)*, IEEE, 2016, pp. 1–6.

[11] T. Nagashima, X. Wei, E. Bou, E. Alarcón, and H. Sekiya, “Analytical design for resonant inductive coupling wireless power transfer system with class-E inverter and class-DE rectifier,” in *2015 IEEE International Symposium on Circuits and Systems (ISCAS)*, IEEE, 2015, pp. 686–689.

[12] R. Vaka and R. K. Keshri, “Design considerations for enhanced coupling coefficient and misalignment tolerance using asymmetrical circular coils for WPT system,” *Arab. J. Sci. Eng.*, vol. 44, pp. 1949–1959, 2019.

[13] S. Hasan, T. Göktaş, and M. Arkan, “Design, Simulation and Application of Buck Converter with Digital PI Controller,” *Balk. J. Electr. Comput. Eng.*, vol. 9, no. 2, pp. 106–113, 2021.

[14] L. Tan *et al.*, “The design and optimization of a wireless power transfer system allowing random access for multiple loads,” *Energies*, vol. 12, no. 6, p. 1017, 2019.

[15] D. Czarkowski and M. K. Kazmierczuk, “ZVS class D series resonant inverter-discrete-time state-space simulation and experimental results,” *IEEE Trans. Circuits Syst. I Fundam. Theory Appl.*, vol. 45, no. 11, pp. 1141–1147, 1998.

[16] D. Iero, R. Carotenuto, M. Merenda, F. Pezzimenti, and F. G. Della Corte, “Performance evaluation of Silicon and GaN switches for a small wireless power transfer system,” *Energies*, vol. 15, no. 9, p. 3029, 2022.